Journal of Power Sources 196 (2011) 5889–5896

Contents lists available at ScienceDirect

Journal of Power Sources

journal homepage: www.elsevier.com/locate/jpowsour

Interaction of sealing material mica with interconnect steel for solid oxide fuel cells application at 600 °C

Martin Bram*, Leszek Niewolak, Nikhil Shah, Doris Sebold, Hans Peter Buchkremer

Forschungszentrum Jülich, Institute of Energy Research, IEF-1: Materials Synthesis and Processing, 52428 Juelich, Germany

ARTICLE INFO

Article history:
Received 16 December 2010
Received in revised form 4 February 2011
Accepted 27 February 2011
Available online 6 March 2011

Keywords:
Sealing SOFC
Mica
Interconnect steel
Oxidation
Intermediate temperature

ABSTRACT

In the last few years, a lot of effort has been undertaken to reduce the operation temperature of solid oxide fuel cells (SOFCs). Intermediate temperatures in the range of 600–650 °C are thought to be highly attractive due to the expected reduction of high-temperature corrosion and interdiffusion phenomena. Furthermore, each stack operated at higher temperatures has to pass this temperature range during thermal cycling. In this work, a study has been carried out to investigate the interaction between interconnect steel (DIN 1.4760) and vermiculite mica paper filled with talc at 600 °C. Mica paper has been implemented recently as a new sealing material for SOFC stacks, aiming to replace established but brittle glass ceramics. Corrosion experiments were conducted at 600 °C under dual gas atmosphere conditions as well as in air. The interconnect steel showed the formation of non-protective oxide scales in contact with mica, especially in the presence of air. The morphology of oxide scales was investigated by SEM/EDX. Possible reasons for this unexpected result are discussed. The complete encapsulation of mica by embossed and welded sheets made of FeCrAlY-steel (DIN 1.4767) as well as the pre-oxidation of interconnect steel were investigated as solutions to this problem. Pre-oxidation was found to be a promising measure to protect the interconnect steel from breakaway oxidation in contact with mica.

1. Introduction

Solid oxide fuel cells (SOFCs) are solid-state energy conversion devices that produce electricity by the electrochemical reaction of an oxidant and a fuel gas at higher temperatures. Stacks of planar SOFCs are believed to offer the potential for higher cost efficiency and power density per unit volume when compared to tubular designs [1]. However, for a high temperature sealing concept, stability and low leakage during long-term operation including thermal cycles remains a crucial challenge. An increase in leak rates reduces the efficiency of the system. Furthermore, large leaks lead to gas-phase oxidation of fuel, forming so-called "hot spots". These can potentially damage SOFC stack components.

Seals in SOFC stacks have to fulfil a variety of requirements [2]. Long-term stable separation of oxidant and fuel gases, even under thermal cycles has to be ensured. Thermochemical and thermomechanical compatibility with the adjacent SOFC components must be realized. The sealing material should also sufficiently compensate the mechanical and thermal mismatch of the stack components, while not affecting or deteriorating the functional layers of the SOFC. Furthermore, electrical insulation is required to avoid short circuits when stacking cells and interconnects.

Currently, glass ceramics are the sealing materials most commonly used. They offer gas tightness and the potential for adapting the coefficients of thermal expansion (CTE) to other stack components by controlling the crystallizing phase content. Typically, the electrical resistance and chemical inertia of glass ceramics are sufficient for SOFC application. However, due to the inherent brittleness and the rigid interfaces, crack growth in the sealant or the sealant/interconnect interface may occur in the case of thermal cycles during stack operation [3–6].

A possible alternative to glasses is the use of compressive, non-bonding seals. If the seals are non-bonding, the individual stack components are free to expand and contract during thermal cycling. The sealing material acts as a gasket, when a sufficient compressive force is applied to the stack [7]. Compressive seals based on mica show a high potential to fulfil this task. Mica is generally known for its high resistivity, uniform dielectric constant/capacitance stability, and low power loss. It is mainly used in electronics devices [8]. Even in commercial mica products, natural micas are used as starting materials. Generally, micas are sheet silica minerals. Their general formula is AB_3 $(X, Si)_4O_{10}$ $(O, F, OH)_2$. In most micas, the A cation is potassium. The B cation can be aluminium, lithium, iron, zinc, chromium, vanadium, titanium, manganese, and/or magnesium. The X ion is usually aluminium, but can also be beryllium, boron and/or iron. Recently, several studies have been conducted

* Corresponding author at: Forschungszentrum Julich GmbH, Institute of Energy and Climate Research IEK-1, Leo Brandt Strasse, D-52425 Julich, Germany.
Tel.: +49 2461 61 68 58; fax: +49 2461 61 24 55.
E-mail address: m.bram@fz-juelich.de (M. Bram).

0378-7753/$ – see front matter © 2011 Elsevier B.V. All rights reserved.
doi:10.1016/j.jpowsour.2011.02.086

to investigate the potential of mica for sealing SOFC stacks [7–14]. To improve the sealing behaviour of commercial mica paper, a novel composite seal has been developed at Forschungszentrum Jülich, where the mica paper is encapsulated by embossed steel sheets, which are subsequently welded to improve gas tightness. Its potential to fulfil the requirements of sealing SOFC stacks has been demonstrated [7].

In the present work, a study was conducted to investigate the oxidation behaviour of different batches of interconnect steel (DIN 1.4760) in contact with mica paper, which was composed of vermiculite filled with talc, at 600 °C. This work was part of the European project "SOFC 600". It is known from a former study that a serious change in the oxidation behaviour of the interconnect steel (DIN 1.4760) may occur if it is annealed in contact with mica under dual gas atmosphere at 800 °C [15]. The occurrence of volatile Mg species of the mica paper, which may be caused by a decomposition of mica components, is proposed to be one of the main reasons for the observation. In the literature, the existence of alkali and potassium ions, which are common elements in natural mica minerals, are also discussed as critical for SOFC operation [16,17]. Before the present investigation, it was expected that anomalous oxidation in the presence of mica would be clearly reduced if the operation temperature was decreased to 600 °C. To confirm this expectation, the oxidation behaviour of interconnect steels in contact with mica was determined in air at 600 °C. In addition, dual gas tests were conducted at 600 °C using the same experimental set-up as in our former study [15]. Due to the unexpected occurrence of breakaway oxidation even at 600 °C, complete encapsulation of the mica paper with laser-welded FeCrAlY-steel sheets (DIN 1.4767), as well as a pre-oxidation of the interconnect steel, were investigated as methods of avoiding breakaway oxidation.

2. Experimental

2.1. Starting materials

Commercial mica paper was used for the study, which combines promising gas tightness with a notable flexibility [18,19]. The raw material is Vermiculite $(K, Mg, Fe)(Si, Al)_4O_{10}(OH)_2$, which is filled with talc (steatite $Mg_3SiO_4O_{10}(OH)_2$) to improve gas tightness at moderate loads. Filling the vermiculite mica with talc reduces the leak rate at a given load by a factor of 10 [15], which advise this material as preferred compared to mica papers without talc.

The steel counterpart was high chromium ferritic steel (DIN 1.4760), which was developed for SOFC interconnects application at Forschungszentrum Juelich [20]. In the study, different batches of this kind of steel were used, which differ in their manufacturing route. Batch LLW was made by vacuum induction melting (VIM), which results in a reduced amount of manufacturing related impurities such as Si and Al. Batch LML was manufactured by conventional melting using Al and Si for de-oxidation. This leads to a notable Al and Si content in the final product. Depending on the final product form (sheet, plate etc.) grain size and grain shape vary from batch to batch. To consider also these factors on high-temperature oxidation in contact with mica, another batch (SC105) was used, which differed in sample thickness and grain size compared to batches LLW and LML. Table 1 summarizes the properties of all batches. Fig. 1 shows their microstructures. The ferritic steels exhibited a recrystallized microstructure consisting of equiaxed ferrite grains, in some cases with precipitates of Ti-rich carbonitrides. One exception was batch LML, which showed a slight texture in the rolling direction. The tested steels showed significant differences in grain size. Batches LML and LLW possessed similar grains sizes with average diameters around 50 μm but a clear difference in grain shape. In contrast, SC105 exhibited significantly bigger grains with the average diameter exceeding 200 μm.

Table 1
Properties of interconnect steel (DIN 1.4760) batches used in this study. LLW was manufactured by conventional melting using Al and Si for de-oxidation, LML and SC105 were manufactured by vacuum induction melting.

Batch	D (mm)	Chemical composition (wt.%)						
		Fe	Cr	Mn	Si	Al	Ti	La
LLW	1	Bal.	22.8	0.45	0.1	0.13	0.08	0.07
LML	1.5	Bal.	22.7	0.42	0.01	0.01	0.07	0.1
SC105	6	Bal.	22.6	0.4	0.02	0.01	0.06	0.12

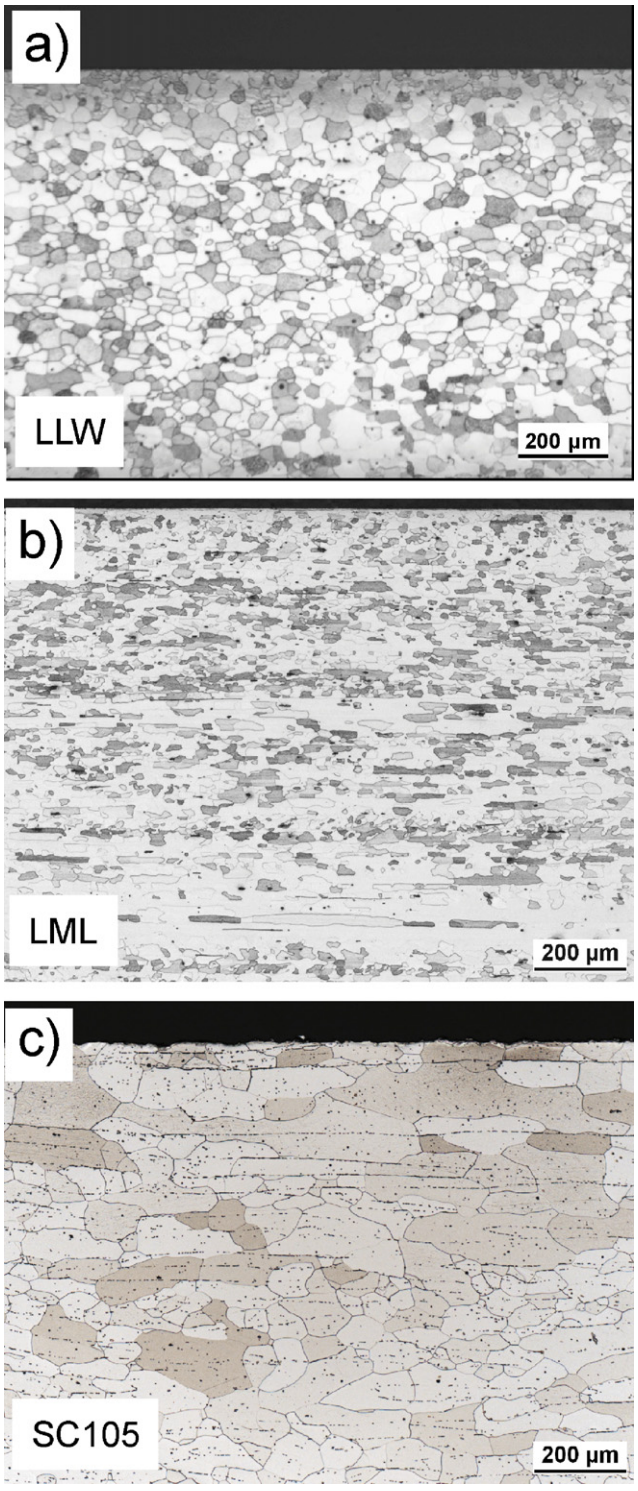

Fig. 1. Microstructures of interconnect steel (DIN 1.4760) batches used in this study (a) LLW, (b) LML and (c) SC105.

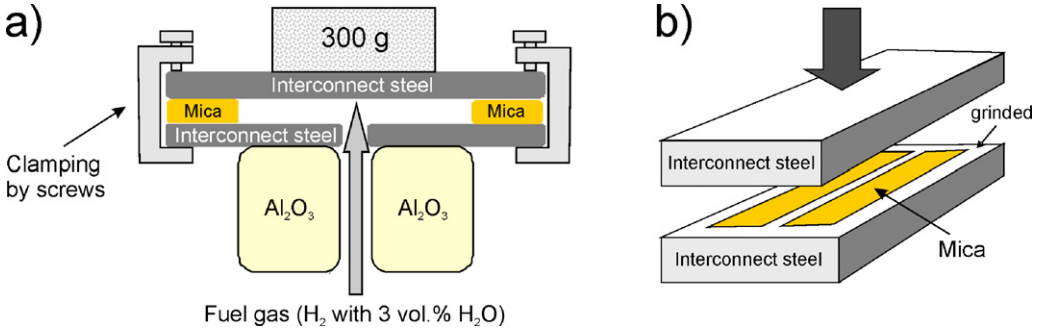

Fig. 2. Schematic illustration of experimental set-up for corrosion experiments in (a) air and (b) dual gas atmosphere.

2.2. Exposition in air

At first, all steel batches were annealed in contact with the mica paper for 400 h at 600 °C in air. Fig. 2a shows the experimental set-up, where two stripes of the mica paper (18 mm × 4 mm × 0.5 mm each) was placed between two steel plates of each batch with varying thickness D (20 mm × 10 mm × D mm). Before mounting the samples, steel surfaces in contact with mica were ground using 1200 SiC grit abrasive paper. The sandwich arrangements were assembled by pressing them in a hand press with 60 MPa to pre-compact the mica inside to a thickness of approximately 0.3 mm. During exposition in air, no external load or clamping by screws was applied. Then, the samples were annealed in air for 400 h at 600 °C.

2.3. Exposition in dual gas atmosphere

Additionally, experiments were performed in dual gas atmosphere at 600 °C for 400 h using the experimental set-up shown in Fig. 2b. All dual gas samples were made from batch SC105. Plates of the size 50 mm × 50 mm × 6 mm were machined. Then, surfaces in contact with mica were ground using 1200 SiC grit abrasive paper. One of the steel plates had a drilled hole of 10 mm diameter in the centre. Mica paper samples were cut to a square geometry of 50 mm × 50 mm, a width of 4 mm and a thickness of 0.5 mm. Mica was pre-compacted with a load of 60 MPa applied by a hand press resulting in a thickness of approximately 0.3 mm. The samples were clamped by two screws tightened with a turning moment of 6 Nm. The specimens were placed in the exposition furnace on an Al_2O_3 ring with polished surfaces. Then, a dead load of 300 g was placed on top of each specimen (Fig. 2b). The furnace was heated up to 600 °C with a rate of 2 K/min in air. The samples were exposed to a dual gas atmosphere, whereby the inner cavity between the two plates was flushed with humidified hydrogen (H_2/3%H_2O), while the outer side was in contact with air. A more detailed description of the experimental set-up is given in [21].

2.4. Protection against breakaway oxidation

To protect the interconnect steel against breakaway oxidation in the presence of mica, two measures were investigated.

Measure 1 - Encapsulation of mica: A complete encapsulation of mica was thought to be suitable to avoid chemical interaction between mica and interconnect steel. Therefore, mica was placed between embossed sheets, which were subsequently gas-tight welded. For encapsulation, a FeCrAlY-steel (DIN 1.4767) sheet with a thickness of 230 μm was used [22]. In preliminary studies, Al_2O_3-forming FeCrAlY-steel did not show any abnormal oxidation when treated in air in direct contact with mica. The compressive mica inlay was a Vermiculite mica paper without talc filler, which was precompressed to a thickness of 800 μm [15]. Fig. 3 shows the principle of this compressive metal/ceramic composite seal. The exposition was carried out at 600 °C for 400 h. To balance a slight distortion of the samples, which occurred during the welding process, the dual gas samples were clamped by four screws, again with a turning moment of 6 Nm for each screw.

Measure 2 - Pre-oxidation: Interconnect steel (Batch SC105) plates were ground with 1200 SiC grit abrasive paper and later pre-oxidized for 24 h at 800 °C in air. Afterwards, pre-compressed Vermiculite mica filled with talc was placed between the pre-oxidized plates. Annealing was done in air as well as in dual gas atmosphere using the same experimental set-ups and parameter sets as given before.

2.5. Microstructural investigation

After exposure, all steel samples were epoxy mounted and cross sectioned. The cross sections were analysed by optical and scanning electron microscopy (SEM). A Zeiss Ultra 55 as well as a Zeiss Supra 35, both equipped with energy dispersive X-ray analysis (Oxford Instruments), were used for SEM investigations. Surface topography of the oxide scales was investigated in the SE-modus (secondary electrons), cross sections of the oxide scales in the BSE-modus (back-scattered electrons). The energy of the electron beam was 15 keV in both cases.

3. Results and discussion

3.1. Exposition in air in contact with mica paper

Interconnect steel oxidized at 600 °C in air formed a thin protective chromia-based scale. A detailed discussion of the oxidation behaviour of this kind of steel can be found elsewhere [23–26]. Fig. 4a and b shows macro pictures of batches LLW and LML oxidized for 400 h at 600 °C in air in contact with mica paper. Under prevailing conditions, batches LML and LLW formed a thin protective chromia-based scale on their surfaces. In addition, plate-like oxides were formed, which were randomly distributed on the surface. This phenomenon was interpreted as the beginning change of the oxidation behaviour (Fig. 4c and d). In contrast, a sample of batch SC105 tested under the same conditions exhibited already

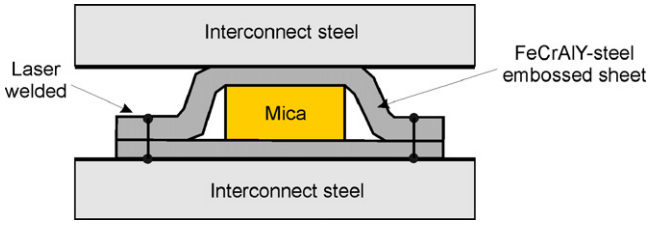

Fig. 3. Principle of compressive metal/ceramic composite seal.

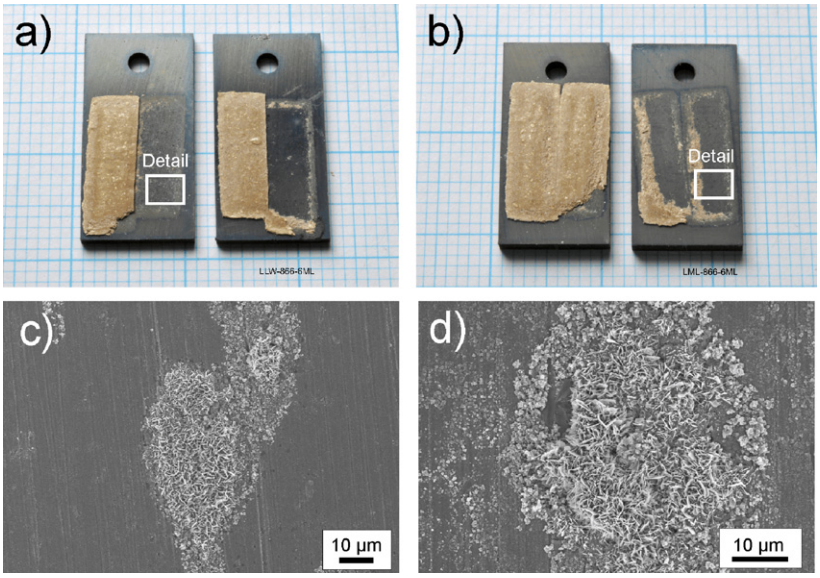

Fig. 4. Batches LLW and LML after exposition in air at 600 °C for 400 h in contact with mica paper, (a and c) batch LLW and (b and d) batch LML. Formation of plate-like oxides indicates the beginning of a change in oxidation behaviour.

a clearly pronounced, dark brown oxide scale on the surface, indicating the formation of a non-protective Fe-rich oxide scale (Fig. 5). Direct contact with mica does not appear to be mandatory to initiate this breakaway oxidation.

A detailed analysis of the multilayered oxide scale formed after exposition in air was conducted by SEM/EDX (Fig. 6). The overall thickness of the oxide scales was approximately 70 μm. The clearly pronounced morphology of each layer enabled quantitative EDX analysis. Results of the quantitative analysis are summarized in Table 2, while the positions of EDX measurements are marked in Fig. 6. In addition, an element mapping of the multilayered oxide scale is shown in Fig. 7. Based on the microstructural analysis, it was concluded that the oxide scale formed on the interconnect steel under prevailing conditions consisted of an outer hematite (Fe_2O_3) layer, an intermediate porous layer of magnetite (Fe_3O_4) and an internal layer mainly containing Fe, Cr-oxide, probably Fe, Cr-spinel $(Cr, Fe)_3O_4$. Furthermore, an internal oxide is marked in Fig. 6, which mainly consists of Cr_2O_3. The formation of finely dispersed oxides of Al, Ti or Si, which could also appear under the given thermodynamic conditions, was not detectable with the experimental set-up used in this study.

3.2. Analysis of mica paper/interconnect steel samples annealed in dual atmosphere

Fig. 8 shows macro pictures of batch SC105 tested in contact with mica paper for 400 h at 600 °C under dual atmosphere conditions. From visual inspection, areas with enhanced corrosion were already clearly visible on the air side (Fig. 8a). This observation was confirmed by metallographical investigation (Fig. 8b and d). The non-protective Fe-rich oxide layer rose to the triple phase boundary air–mica–steel as shown in Fig. 8b. Enhanced oxidation obviously started from a complete oxidation of single grains, which can occur far away from the triple phase boundary mica–steel–air (Fig. 8d). The thickness of the Fe-rich oxide scale was again approximately 70 μm. In contrast, at the mica–steel interface a thin protective chromia-based scale was formed (Fig. 8c). The same result was found on the anode side (not shown here).

Almost the same results were achieved, when the dual gas tests of interconnect steel were conducted in presence of a Phlogopite mica paper, which did not contain a filler material. This material has also been used in recent studies to seal SOFC stacks [14,15]. A detailed discussion of the results is omitted here.

Table 2
Results of quantitative EDX analysis of the multilayered oxide scale. Contents are given in at.%.

Spectrum	O	Cr	Fe
1	60.6	–	39.4
2	56.6	–	43.4
3	57.2	–	42.4
4	58.7	20.1	21.2
5	57.3	21.6	21.1
6	58.0	21.3	20.8

3.3. Protection against breakaway oxidation–encapsulation of mica

A first attempt to overcome the enhanced oxidation of the interconnect steel in contact with mica was a complete encapsulation of mica by embossed steel sheets, which were subsequently welded to improve gas tightness. FeCrAlY-sheets were used to manufacture this composite seal. Fig. 9 shows the samples after exposition under dual atmosphere conditions at 600 °C for 400 h. Generally, on a macroscopic scale, the surface covered by non-protective oxide scale on the air side was reduced, however, some breakaway spots could still be found (Fig. 9c). Furthermore, enhanced oxidation was also found on the contacts between FeCrAl- and interconnect steel (Fig. 9d).

3.4. Protection against catastrophic oxidation–pre-oxidation of the interconnect steel

The most promising attempt to protect the interconnect steel from breakaway oxidation in contact with mica was a controlled pre-oxidation of the steel in air at 800 °C for 24 h. Fig. 10 shows the dual gas sample consisting of mica paper in contact with pre-oxidized batch SC105 after exposition at 600 °C for 400 h. A detailed microstructural investigation of the oxide scale formed under the above mentioned conditions was disclaimed in this study. The morphology of the duplex-oxide layer formed on the interconnect steel

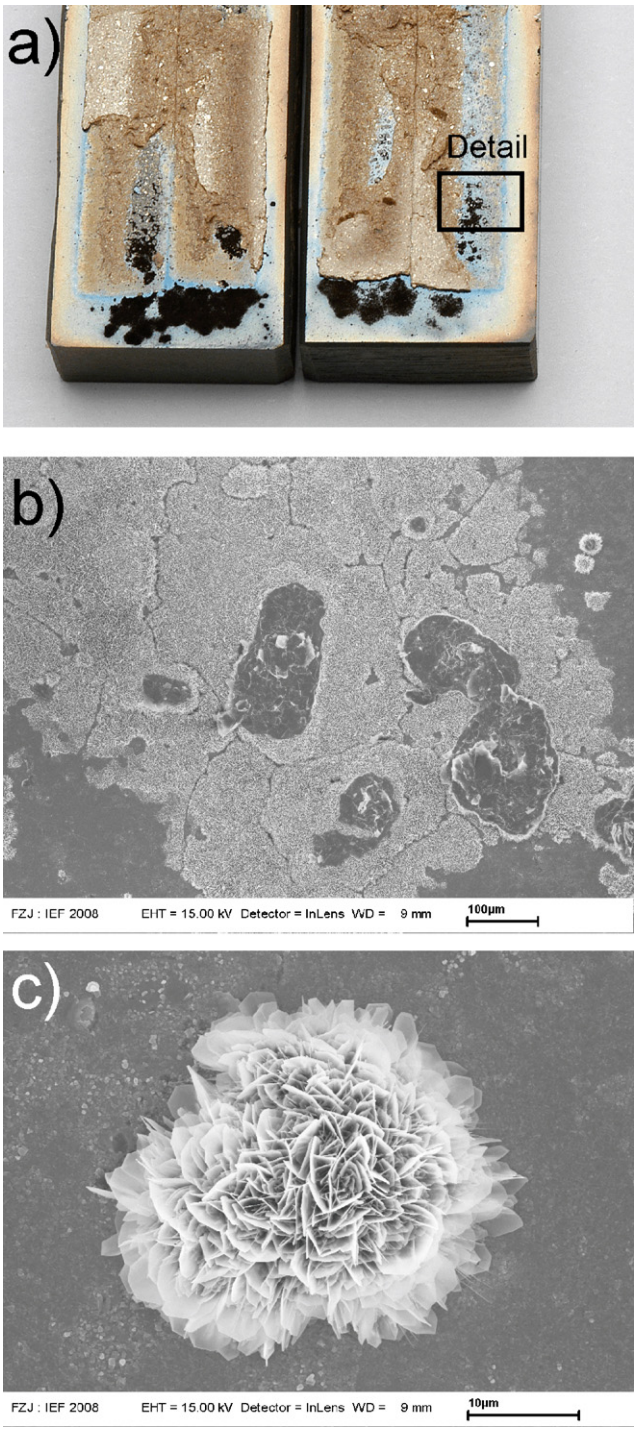

Fig. 5. Batch SC105 after exposition in air for 400 h at 600 °C in contact with mica paper. (a) Overview, dark brown oxide scale indicates the onset of breakaway oxidation, (b) microstructure of brown dots and (c) detail. (For interpretation of the references to color in this figure legend, the reader is referred to the web version of this article.)

(DIN 1.4760) during pre-oxidation at 800 °C in air can be found elsewhere [23]. Pre-oxidation treatment seems to reliably avoid any breakaway oxidation. Neither on the air nor on the anode side was any breakaway oxidation found (Fig. 10b). For confirmation of the result, the experiment was repeated in air using the same experimental set-up as described in Section 2.2. Again, pre-oxidation reliably protected against breakaway oxidation for at least 400 h (results not shown here).

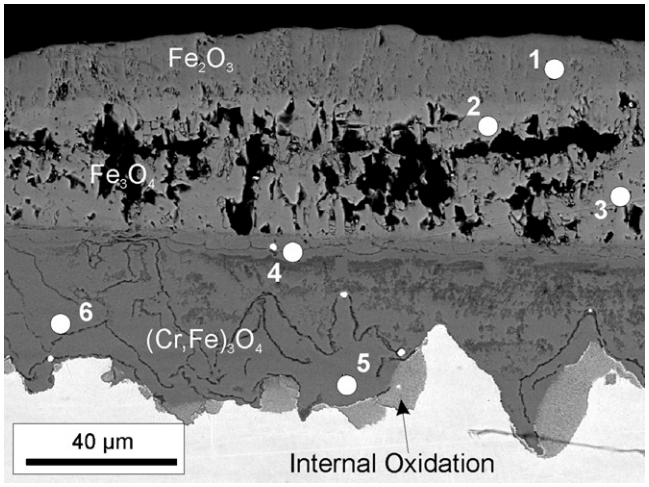

Fig. 6. Microstructure of the multiscaled oxide layer on the interconnect steel (Batch SC105) and positions of EDX analysis. Results of EDX analysis see Table 2.

3.5. Discussion of the results

The results of oxidation experiments show that the coarse-grained batch SC105 is generally more susceptible to breakaway oxidation than batches LLW and LML. In the case of this batch, only proper pre-oxidation can sufficiently protect the steel. As investigated in Section 3.3 even completely separating the steel from mica by complete encapsulation in FeCrAlY-steel sheets envelope did not prevent the local appearance of enhanced oxidation. This suggests that mica must not necessarily be present to induce enhanced oxidation of the steel at 600 °C in air.

Nevertheless, it is obvious – especially for batch SC105 – that the presence of mica supports enhanced oxidation. It is notable that direct contact of both materials is not required to induce breakaway oxidation. Strongly corroded parts of the specimen were mostly away from the mica/steel interface. This result suggests that volatile species are involved in enhanced oxide formation. In an earlier study, the decomposition of Vermiculite mica filled with talc was investigated by DTA/TGA in combination with XRD [15]. Even if this study was focused on application of mica at 800 °C, some conclusions can be also drawn for the present investigation. During heating with a ramp of 5 K/min to 600 °C in air, a weight loss of 1.8 wt.% was observed. The weight loss in this temperature range is mainly caused by the evaporation of water probably due to the dehydration of hydrated vermiculite, which was detected in the starting material by XRD. If continuing the heating process to higher temperatures, the decomposition of talc to enstatite, silica and water was indicated by a strong weight loss above 810 °C, which is coupled with two endothermic peaks in the temperature range between 810 °C and 950 °C. Fully dehydration of hydrated vermiculite as well as fully decomposition of talc were confirmed by subsequent XRD measurements. MacKenzie et al. published results on the decomposition of natural talc [27], which support the results of our former investigation. In his study, decomposition started not before 875 °C. From these results, we conclude that the oxidation of Crofer 22 APU at 600 °C is mainly influenced by the evaporation of water from mica. Even if the decomposition of talc seems to be negligible at 600 °C, the occurrence of volatile alkaline and earthalkaline species could not be precluded definitely at this temperature and requires further investigations. However, volatile species cannot explain the results obtained with mica encapsulated by FeCrAlY-steel. In summary, the presence of volatile alkali species might enforce enhanced oxidation at 600 °C, but it cannot be the only reason for this behaviour.

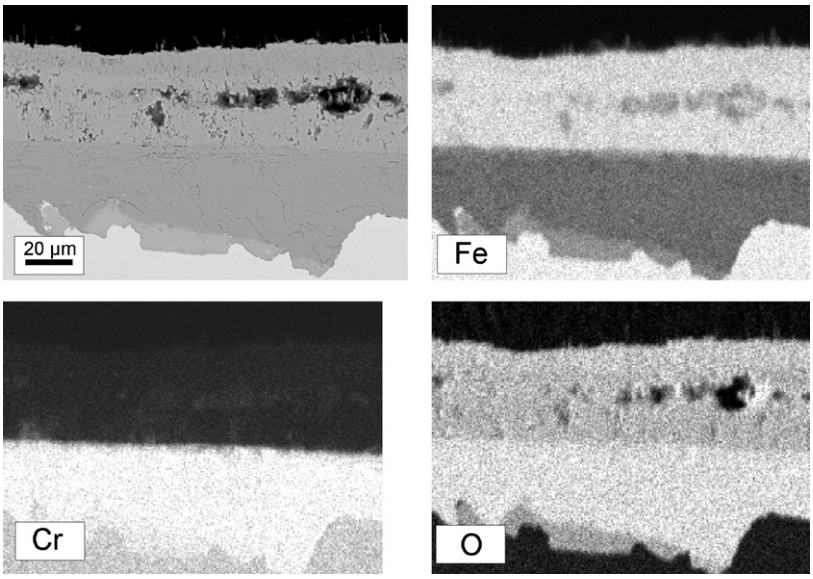

Fig. 7. Element mapping of the multilayered oxide scale.

The oxidation of the interconnect steel for a few hundred hours at 600 °C in laboratory air is characterized by the formation of a protective chromia-based scale with a thickness below 500 nm [26]. According to the Wagner theory, to maintain the protective character of the scale, the supply of scale-forming element (e.g. Cr) to the metal/oxide interface must compensate its consumption by the growing oxide [28]. Increased consumption of chromium or its limited supply may result in breakaway corrosion manifested by the formation of non-protective Fe-oxide-based scale.

One of the possible reasons for enhanced chromium consumption can be its evaporation. According to data presented in [29], Cr-release from the interconnect steel (DIN 1.4760) at 600 °C in wet air (air + 2%H_2O) is about 4.5×10^{-11} kg m^{-2} s^{-1}. Chromium release in wet atmospheres with high oxygen partial pressures appears mainly by volatile $CrO(OH)_2$ species. In other words, increasing air humidity over chromia scale results in an enhanced chromium evaporation rate due to the formation of volatile $CrO(OH)_2$. In the present study, the thermally induced decomposition of mica and/or micro leaks in the case of dual atmosphere experiments could be responsible for a local increase of water provoking breakaway oxidation. Breakaway oxidation induced by chromium evaporation is well documented for a number of ferritic and austenitic steels [30–32]. Time to breakaway decreases with increased water content in the gas [33]. Generally, ferritic steels should be less susceptible to such effects due to the higher Cr-diffusivity in the ferrite matrix compared to those in an austenitic matrix [34,35]. However, at relatively low temperatures (e.g. 600 °C), diffusion processes are mainly controlled by microstructural features such as grain boundaries and/or dislocations. Therefore, steels with larger grains (lower grain boundary density) should be more susceptible to chromium-evaporation-induced breakaway oxidation. Indeed, the presented data seems to confirm this statement. Fine-grained steels (batches

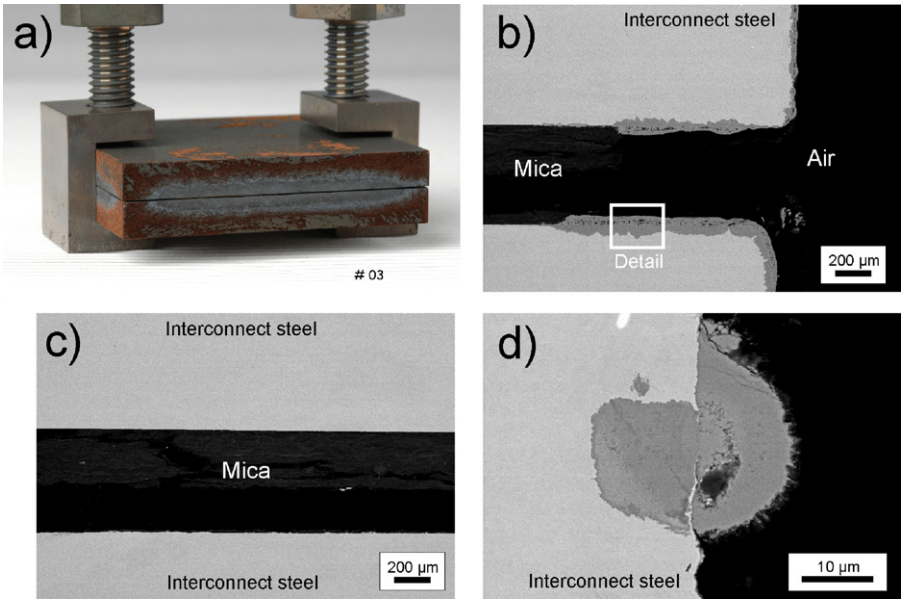

Fig. 8. Enhanced oxidation of the outer surface of interconnect steel (Batch SC105) after annealing under dual gas atmosphere in contact with mica paper for 400 h at 600 °C (a) visual view, (b) cross section of the air side with severe oxidation, (c) formation of thin protective chromia scale at the interface mica–steel and (d) breakaway oxidation obviously starts from single grains without direct contact with mica.

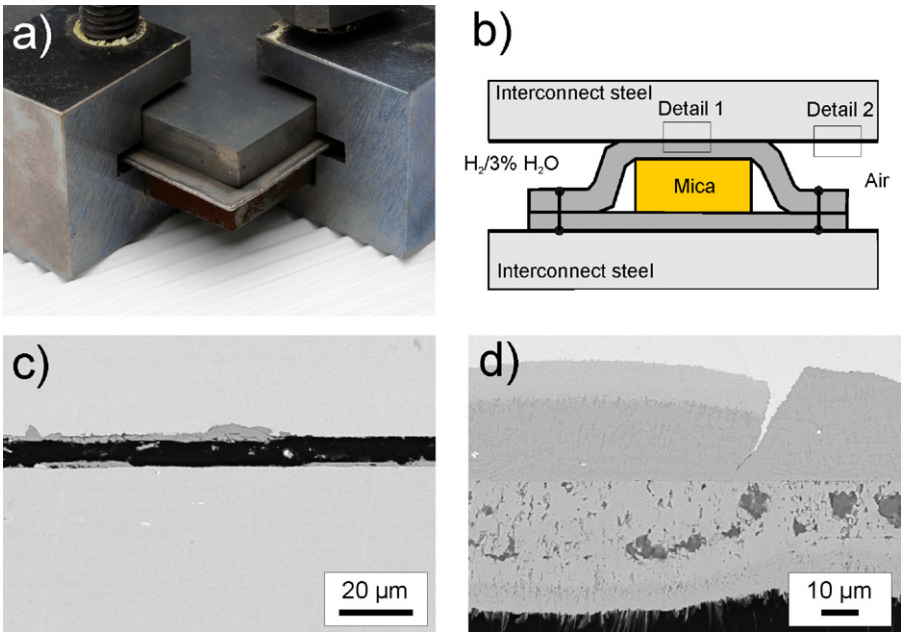

Fig. 9. Composite seal (mica paper encapsulated by FeCrAlY-steel) in contact with the interconnect steel (Batch SC105) after exposition for 400 h at 600 °C in dual atmosphere (a) visual view, (b) positions of metallographic analysis, (c) detail 1: beginning of oxidation at the contact area between FeCrAlY- and interconnect steel; the gap is caused by metallographical preparation and (d) detail 2: enhanced oxidation on the air side.

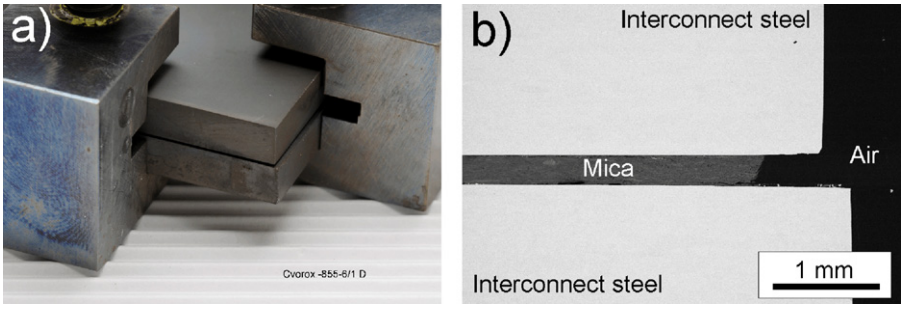

Fig. 10. Cross-section of pre-oxidized interconnect steel (Batch SC105) in contact with mica paper after exposition in dual gas atmosphere at 600 °C for 400 h. No anomalous oxidation of the interconnect steel was found (a) visual view, (b) cross section.

LLW and LML) oxidized under prevailing conditions formed protective oxide scales and virtually no evidence of breakaway oxidation was found. In addition, a clear influence of the Al and Si content on the oxidation seems to be negligible under the given conditions. In the case of coarse-grained steels, proper pre-oxidation seems to be a very effective way of preventing breakaway corrosion as demonstrated for the SC105 batch. Sufficiently thick chromia-based scale formed during the pre-oxidation process can effectively protect the steel even if it is partly removed by evaporation. Former studies reveal that such layer is also suitable to withstand stresses occurring during thermal cycling [23,36].

4. Conclusions

Mica paper is a promising sealing material for SOFC stacks, which requires a permanent load to achieve gas tightness. Due to its compressive, non-bonding character, it allows the individual stack components to expand and contract freely during thermal cycles, reducing the influence of TEC mismatch on stack performance. It is known from earlier studies that the presence of mica might influence the formation of protective oxide scales on SOFC interconnect steel (DIN 1.4760) at SOFC operation temperature (800 °C). In the present study, comparable experiments were conducted at 600 °C, with an operation of SOFC at intermediate temperatures in mind.

Different batches of SOFC interconnect steel (DIN 1.4760), which varied in grain size, thickness and Al and Si contents, were exposed to direct contact with Vermiculite mica paper, which was filled with talc, for 400 h at 600 °C in air. The formation of non-protective Fe-based oxide scales was detected, indicating breakaway oxidation, especially in the case of coarse grains (batch SC105). Reducing the alloy grain size (batches LLW and LML) resulted in the formation of a thin protective chromia-based oxide scale. Nevertheless, the formation of randomly distributed, plate-like oxide scales also indicated the beginning of a change in the oxidation behaviour for these batches.

In addition, samples from coarse-grained batch SC105 were exposed to contact with abovementioned mica paper under dual gas conditions for 400 h at 600 °C. Samples showed the formation of thick, non-protective oxide scales, preferentially on the air side. This oxidation starts from single grains. A direct contact of the steel surface to mica was not mandatory to initiate breakaway oxidation, therefore indicating that gas phase transport processes can be responsible for the observed effects.

The appearance of breakaway oxidation can be connected with a combination of steel microstructure and locally increased air humidity, e.g. by the dehydration of hydrated Vermiculite. Coarse-grained steel microstructure and increased air humidity tend to increase the susceptibility to breakaway oxidation. The presence

of volatile earthalkali or alkali species, caused for example by a partial decomposition of mica, could further enhance the tendency to breakaway oxidation at 600 °C, but it does not appear to be the main reason.

Two measures were investigated to protect the interconnect steel from breakaway oxidation in the presence of mica: (a) a complete encapsulation of mica by embossed and gastight-welded FeCrAlY-steel (DIN 1.4767) sheets, (b) a pre-oxidation of the interconnect steel in air at 800 °C for 24 h. While the encapsulation did not solve the corrosion problem (a non-protective oxide scale was still present on the air side), pre-oxidation was found to be most promising if mica is used as sealing material for SOFC stacks. Pre-oxidation leads to the homogeneous formation of a protective chromia-based oxide scale on the steel surface, which reliably avoids breakaway oxidation in the presence of mica for at least 400 h.

Acknowledgements

The authors are grateful for financial support from the European Commission under contract No. SES6-2006-020089 (SOFC600). They also would like to thank B. Hausmann for manufacturing composite samples, V. Haanappel for conducting the experiments in the dual environment, M. Kappertz for helping in metallographic preparation, H. Moitroux for taking macro pictures and E. Wessel for SEM/EDX investigations. We would also like to thank W.J. Quadakkers for helpful discussions.

References

[1] S.C. Singhal, Solid State Ionics 152–153 (2002) 405–410.
[2] J.W Fergus, J. Power Sources 147 (2005) 46–57.
[3] K.L. Ley, M. Krumpelt, R. Kumar, J.H. Meiser, I. Bloom, J. Mater. Res. 11 (1996) 1489–1493.
[4] N. Lahl, L. Singheiser, K. Hilpert, K. Singh, D. Baradur, J. Mater. Sci. 35 (2000) 3089–3096.
[5] Z. Yang, J.W. Stevenson, K.D. Meinhardt, Solid State Ionics 160 (2003) 213–225.
[6] Y.S. Chou, J.W. Stevenson, P. Singh, J. Power Sources 184 (2008) 238–244.
[7] M. Bram, S. Reckers, P. Drinovac, J. Mönch, R.W. Steinbrech, H.P. Buckkremer, D. Stöver, J. Power Sources 138 (2004) 111–119.
[8] S.P. Simner, J.W. Stevenson, J. Power Sources 102 (2001) 310–316.
[9] Y.S. Chou, J.W. Stevenson, J. Power Sources 140 (2005) 340–345.
[10] Y.S. Chou, J.W. Stevenson, J. Power Sources 191 (2009) 384–389.
[11] M. Bram, S. Reckers, P. Drinovac, J. Mönch, R.W. Steinbrech, H.P. Buchkremer, D. Stöver, Proc. Electrochem. Soc. (SOFC VIII), 2003–2007, 2003, pp. 888–897.
[12] S. Le, K. Sun, N. Zhang, M. An, D. Zhou, J. Zhang, D. Li, J. Power Sources 161 (2006) 901–906.
[13] S. Le, K. Sun, N. Zhang, Y. Shao, M. An, Q. Fu, X. Zhu, J. Power Sources 168 (2007) 447–452.
[14] M. Rautanen, O. Himanen, V. Saarinen, J. Kiviaho, Fuel Cells 5 (2009) 753–759.
[15] F. Wiener, M. Bram, H.P. Buckkremer, D. Sebold, J. Mater. Sci. 42 (2007) 2643–2651.
[16] R. Weiss, D. Peck, M. Miller, K. Hilpert, in: F.W. Poulsen, N. Bonanos, S. Linderoth, M. Mogensen, B. Zachau-Christiansen (Eds.), High Temperature Electrochemistry: Ceramics and Metals, Proceedings of the 17th Risø International Symposium on Materials Science, Risø National Lab, Roskilde, Denmark, 1996, pp. 479–484.
[17] I.W. Cavel, M.G. Nicholas, J. Nucl. Mater. 95 (1980) 145–154.
[18] Fuel Cells Bulletin (2007) 11.
[19] J. Hoyes, S. Bond, Sealing Technol. 8 (2007) 11–14.
[20] R. Hodja, R. Heimann, W.J. Quadakkers, ThyssenKrupp Tech-forum (2003) 20–23.
[21] V.A.C. Haanappel, V. Shemet, I.C. Vinke, W.J. Quadakkers, J. Power Sources 141 (2005) 102–107.
[22] Krupp VDM GmbH Aluchrom YHf Material Data Sheet No. 8003, November 2001 Edition.
[23] P. Huczkowski, V. Shemet, J. Piron-Abellan, L. Singheiser, W.J. Quadakkers, N. Christiansen, Mater. Corros. 55 (2004) 825–830.
[24] W.J. Quadakkers, V. Shemet, L. Singheiser, U.S. Pat. 2,003,059,335, (2003).
[25] J. Piron, J.P. Abellan, V. Shemet, F. Tietz, L. Singheiser, W.J. Quadakkers, A. Gil, Electrochem. Soc. Ser. 16 (2001) 811–819.
[26] L. Niewolak, E. Wessel, L. Singheiser, W.J. Quadakkers, Potential suitability of ferritic and austenitic steels as interconnect materials for solid oxide fuel cells operating at 600 °C, J. Power Sources 195 (2010) 7600–7608.
[27] K.J.D. MacKenzie, R.H. Meinhold, Thermochim. Acta 244 (1994) 195–203.
[28] P. Kofstad, High Temperature Corrosion, Elsevier, ISBN 1-85166-154-9.
[29] L. Niewolak, W.J. Quadakkers, Report European project "SOFC600 (Contract SES6-2006-020089)", Work Package 2.1: Demonstration of SOFC Stack Technology for Operation at 600 °C, 2010.
[30] W.J. Quadakkers, T. Olszewski, J. Piron-Abellan, L. Singheiser, Oxidation of metallic materials in simulated CO_2/H_2O-rich service environments relevant to an oxyfuel plant. VDI-Berichte 2102, VDI Verlag, (2010) 81–104, ISBN 978-3-18-092102-0.
[31] H. Asteman, J.E. Svensson, L.G. Johansson, Corros. Sci. 44 (2002) 2635–2649.
[32] M. Halvarsson, J.E. Tang, H. Asteman, J.E. Svensson, L.G. Johansson, Corros. Sci. 48 (2006) 2014–2035.
[33] X. Peng, J. Yan, Y. Zhou, F. Wang, Acta Mater. 53 (2005) 5079–5088.
[34] S. Leistikow, I. Wolf, H.J. Grabke, Mater. Corros. 38 (1987) 556–562.
[35] E. Essuman, G.H. Meier, J. Zurek, M. Haensel, W.J. Quadakkers, Oxid. Met. 69 (2008) 143–162.
[36] A. Galerie, F. Toscan, M. Dupeux, J. Mougin, G. Lucazeau, C. Valot, A.M. Huntz, L. Antoni, Mater. Res. 7 (2004) 81–88.